SUPPLEMENTARY DATA

A thermogenic-like brown adipose tissue phenotype is dispensable for enhanced glucose tolerance in female mice

Nathan C. Winn[1,2], Rebeca Acin-Perez[3], Makenzie L. Woodford[1], Sarah A. Hansen[4], Megan M. Haney[4], Lolade A. Ayedun[1], R. Scott Rector[1,5,6], Victoria J. Vieira-Potter[1], Orian S. Shirihai[3], Harold S. Sacks[3], Jill A. Kanaley[1], Jaume Padilla[1,7,8]

[1]Nutrition and Exercise Physiology, University of Missouri, Columbia, MO, USA
[2]Molecular Physiology and Biophysics, Vanderbilt University, Nashville, TN, USA
[3]Division of Endocrinology, Department of Medicine, and Department of Molecular and Medical Pharmacology, David Geffen School of Medicine at UCLA, Los Angeles, CA, USA
[4]Office of Animal Resources, University of Missouri, Columbia, MO, USA
[5]Department of Medicine-Gastroenterology and Hepatology, University of Missouri, Columbia, MO, USA
[6]Research Service-Harry S Truman Memorial VA Hospital, Columbia, MO, USA
[7]Dalton Cardiovascular Research Center, University of Missouri, Columbia, MO, USA
[8]Child Health, University of Missouri, Columbia, MO, USA

Experimental Procedures

Animal surgeries

Surgical procedures were performed for *Experiment 1* and *Experiment 2*. Mice were anesthetized with isoflurane (induction 5%, maintenance 2-3% with room air) and placed in sternal recumbency on a heated surgical pad. A midline skin incision was made along the cranial dorsal surface to reveal the left and right interscapular brown adipose tissue (iBAT) pads. After the initial incision, a dissecting microscope was used to improve visualization and accuracy. *Experiment 1*: Four 5µl injections of adeno-associated virus (AAV) vectors were administered, spread equally throughout the respective tissue. *Experiment 2*: For denervation procedures, to visualize the intercostal nerves beneath the fat pad, the caudal portion of one of the iBAT pads was grasped and gently reflected laterally and cranially while bluntly dissecting connective tissue on the ventral surface. The five most cranial intercostal nerves were identified and gently isolated by blunt dissection. A 2-mm section of nerves was resected to prevent nerve regeneration. The incision was closed using absorbable sutures. All mice were given buprenorphine, 0.05 mg/kg subcutaneously prior to recovery.

Body composition

Percent body fat, fat mass, and lean mass were measured by a nuclear magnetic resonance imaging whole-body composition analyzer (EchoMRI 4in1/1100; Echo Medical Systems, Houston, TX) on conscious mice within two days prior to sacrifice.

Energy expenditure

Using a metabolic monitoring system (Promethion, Sable Systems Int., Las Vegas, NV), energy expenditure and spontaneous activity during the 12-hour light and 12-hour dark cycles were determined by monitoring oxygen consumption and carbon dioxide production over a three-day period, as previously described (1). Energy expenditure is presented as kcal/h/mouse.

Glucose tolerance testing

Glucose tolerance tests were performed at the same environmental temperature at which mice were housed. Briefly, after a five-hour fast, blood glucose was measured from the tail vein. The tail was nicked and blood was sampled by a glucometer (Alpha Trak, Abbott Labs). A baseline measure of blood glucose was taken prior to giving a sterile solution of 50% dextrose (2g/kg body weight (BW)) via

ip injection, as previously performed (2). Glucose measures were taken 15, 30, 45, 60 and 120 minutes after the glucose injection. Glucose total area under curve was calculated using the trapezoidal rule.

Cold tolerance testing

Cold tolerance testing was performed three weeks prior to sacrifice. A rectal probe was inserted (2 to 2.5 cm) into the rectum for approximately 15 seconds to obtain a stable measurement of colonic temperature (Indus Instruments MouseMonitor S, Webster, TX). Following baseline rectal measurements in the animal's ambient environment (28˚C or 20°C), mice were transported to an environmentally-controlled walk-in cooler (4˚C) and singly-housed in 5x3x3" cages with minimal bedding material. Serial measurements of rectal temperature were taken every 30 minutes for 180 minutes. Following the test, mice were transported back to their home cages and warmed with a heating pad for 30 minutes. In a subset of mice, thermal images were taken in the animal's ambient environment and during the cold challenge using a thermal imaging camera (FLIR A315, FLIR Systems, Inc. Wilsonville, OR, USA) to qualitatively assess regional heat emission.

Confocal microscopy

Fresh tissue lysates were collected in 1xPBS prior to microscopy. Whole-tissue lysates (20-100 mg) were placed in a 35-mm glass-bottom imaging dish filled with PBS and imaged with a Leica TCP SP8 inverted laser scanning confocal microscope. GFP fluorescence was excited with a 488 nm laser line and emission was recorded using a 500-550 nm bandpath. Confocal transmitted light images of tissue were recorded simultaneously. Adipocytes and lipid droplets were evaluated using a 20x objective with 1x and 2.75x zoom factors for both BAT and white adipose tissue (WAT) samples.

Immunohistochemistry

Formalin-fixed adipose tissue samples were processed through paraffin embedment, sectioned at 5 µm, and stained with either perilipin, macrophage marker Mac-2 antibody or Hematoxylin & Eosin (H&E) by a commercial laboratory (IDEXX Bioanalytics, Columbia, MO, USA). Antibody information is listed in **Suppl Table 1**. Sections were evaluated via an Olympus BX34 photomicroscope (Olympus, Melville, NY) and images were taken via an Olympus SC30 Optical Microscope Accessory CMOS color camera. Objective quantification of macrophage infiltration in BAT was done by determining the positive Mac-2 stained area per 20x fields of view using Image J software (NIH public domain; National Institutes of Health, Bethesda, MD) (3). All histological assessments were performed by an investigator whom was blinded to the groups.

Transmission electron microscopy

Primary fixation of BAT was performed immediately postharvest in 2% paraformaldehyde, 2 % glutaraldehyde in 100 mM sodium cacodylate buffer pH=7.35. Next, fixed tissues were rinsed with 100 mM sodium cacodylate buffer, pH 7.35 containing 130 mM sucrose. Secondary fixation was performed using 1% osmium tetroxide (Ted Pella, Inc. Redding, California) in cacodylate buffer using a Pelco Biowave (Ted Pella, Inc. Redding, California) operated at 100 Watts for 1 minute. Specimens were next incubated at 4 ^{o}C for one hour, then rinsed with cacodylate buffer and further with distilled water. En bloc staining was performed using 1% aqueous uranyle acetate and incubated at 4^{o}C overnight, then rinsed with distilled water. A graded dehydration series was performed using ethanol at 4°C, transitioned into acetone, and dehydrated tissues were then infiltrated with Epon resin for 24 hours at room temperature and polymerized at 60°C overnight. Sections were cut to a thickness of 85 nm using an ultramicrotome (Ultracut UCT, Leica Microsystems, Germany) and a diamond knife (Diatome, Hatfield PA). Images were acquired with a JEOL JEM 1400 transmission electron microscope (JEOL, Peabody, MA) at 80 kV on a Gatan Ultrascan 1000 CCD (Gatan, Inc, Pleasanton, CA) at the Electron Microscopy Core Facility, University of Missouri.

SUPPLEMENTARY DATA

RNA extraction and quantitative real-time RT-PCR

BAT was homogenized in TRIzol solution using a tissue homogenizer (TissueLyser LT, Qiagen, Valencia, CA). Total RNA was isolated according to the Qiagen's RNeasy lipid tissue protocol and assayed using a Nanodrop spectrophotometer (Thermo Scientific, Wilmington, DE) to assess purity and concentration. First-strand cDNA was synthesized from total RNA using the iScript Reverse Transcription Supermix for RT-qPCR (BioRad, Hercules, CA). Quantitative real-time PCR was performed as previously described using the ABI StepOne Plus sequence detection system (Applied Biosystems) (2). A 20 µL reaction mixture containing 10 µL iTaq UniverSYBR Green SMX (BioRad, Hercules, CA) and the appropriate concentrations of gene-specific primers plus 4 µL of cDNA template were loaded in a single well of a 96-well plate. Gene primer sequences are reported in **Suppl Table 2**. PCR reactions were performed in duplicate under thermal conditions as follows: 95ºC for 10 min, followed by 40 cycles of 95ºC for 15 s and 60ºC for 45 s. A dissociation melt curve analysis was performed to verify the specificity of the PCR products. 18S was used as house-keeping control gene. mRNA expression values are presented as $2^{\Delta CT}$ whereby ΔCT = 'house-keeping' CT - gene of interest CT. mRNA levels were expressed as fold change relative to the control condition per experiment, which was set at 1.

Ex vivo lipolysis

BAT lysates were excised and cut into ~10 mg pieces and placed in 0.297 ml Dulbecco's modified eagle medium (DMEM, 1x, 1g/l glucose, 110mg/l sodium pyruvate) with 2% FFA-free BSA for 15 minutes at 37°C. Thereafter, isoproterenol (ISO, 10 µM) or PBS was added to media and incubated at 37°C for 2 hours under agitation. Following incubation, tissue lysates were removed, briefly washed with PBS, and flash frozen in liquid nitrogen until further analysis. The incubation media was collected and stored at -80°C for assessment of Glycerol (Millipore Sigma). Glycerol is presented as mmol per g of tissue.

Respirometry measurements

BAT tissue lysates were excised, rinsed with 1%PBS, flash frozen in liquid nitrogen, and stored at -80°C until further analyses. Samples were pooled within group (i.e., BAT from two mice within group = one biologic sample within the same group) to yield five biologic samples per group. BAT was homogenized in MAS buffer (70 mM Sucrose, 220 mM Mannitol, 5mM KH_2PO_4, 5 mM $MgCl_2$, 1 mM EGTA, 2 mM HEPES) in a Teflon homogenizer. Samples were spun for ten minutes at 1,000 g at 4°C to remove nuclear and membrane debris. Supernatant was used for frozen respirometry assays in a XFe96 Seahorse equipment. Homogenates (8 µg per well in 20µl volume, minimum of four replicas per condition) were loaded in a XFe 96 well plate and centrifuge at 2,000 x g for 5 min at 4°C using plate carrier rotating buckets in order to adhere mitochondrial particles to the bottom of the plate, with no brake. After centrifugation, 130 µL MAS plus cytochrome c (10 µg/ml final concentration) was added per well. Respirometry assay was performed by serial injections of: NADH or Succinate-Rotenone (1 mM and 5 mM-2 µM final concentration, respectively) in port A; Antimycin A (5 µM final concentration) in port B; TMPD/Ascorbate (0.5mM/1mM final concentration) in port C and azide (50 µM final concentration) in port D. Oxygen consumption rates (OCR) were calculated as the substrate minus inhibitor dependent rates per µg of tissue homogenate.

Citrate synthase activity

Citrate synthase activity was determined using methods from Srere (4). Briefly, BAT homogenates were incubated in the presence of oxaloacetates, acetyl-CoA, and DTNB. Spectrophotometric detection of reduced DTNB served as an index of enzyme activity at a wavelength of 405nm. Data are presented as nmol/min/µg protein.

SUPPLEMENTARY DATA

Immunoblotting

Immunoblotting was performed on adipose tissue lysates including BAT, gonadal WAT, and inguinal WAT as previously described (5). The same amount of protein was loaded within each respective tissue across gels. Antibody information is listed in **Suppl Table 1**. Intensity of individual protein bands were quantified using FluoroChem HD2 (AlphaView, version 3.4.0.0), and expressed as a ratio to β-tubulin or total protein stain (1% amido-black; Sigma-Aldrich). Values are expressed as fold-difference.

Proteomics

BAT samples were homogenized in SDS PAGE sample buffer (1X Laemmli) using a handheld homogenizer (Fisher Scientific, cat. No. 15340172) and following centrifugation (16 K x g), the supernatant was transferred to a fresh tube and protein precipitated with acetone (6). Protein pellets were resuspended in urea buffer (6 M urea, 2 M thiourea, 100 mM ammonium bicarbonate, pH 7.8), protein quantified using the EZQ assay (Invitrogen/Life Tech), and equal amounts (25 ug) of each sample digested overnight with trypsin using a standard in-solution digestion protocol (7). Peptides were then purified using large-format C18 tips according to the manufacturer's protocol (Pierce), lyophilized, and resuspended at 1ug/uL.

LCMS

Peptides were analyzed on a Bruker timsTOF-PRO using the PASEF method (8). Briefly, peptides were loaded onto a C8 Pepmap100 u-precolumn (Thermo) and separated using a 70 min gradient on a nanoElute15 analytical column (15 cm x 75 μm x 1.9 μm ReprosilAQ C18; Bruker Daltonics). The nanoElute LC system is connected to a timsTOF-PRO mass spectrometer using the Captive Spray source (Bruker). MS and MSMS data were acquired using the parallel accumulation-serial fragmentation (PASEF) method with a collection rate of 10 PASEF frames per cycle (~1.7 sec) which results in approximately 120 MSMS spectra per cycle. Data were searched against the NCBInr database limited to Mus sequences (321,035 entries, last update 7/23/2018) using PEAKS V8.5 (Bioinformatics Solutions Inc. Waterloo, ON, Canada) using the following parameters: trypsin as enzyme; 2 missed cleavages allowed; 50ppm mass error tolerance on precursors, 0.05Da error on MSMS fragments; carbamidomethyl-Cys, fixed modification; oxidized Met, variable mod. Following database search, data were filtered to 1% protein FDR using PEAKSDB and protein identification data (including peptide spectral matches, PSMs) exported as an excel file.

Label fee protein quantification

The samples were grouped as follows WD, WD+WR, and CD with 8 samples per group and subjected to label-free quantitation, based on MS1 peak integration, using PEAKS LFQ (PEAKs V8.5, Bioinformatics Solutions Inc. Waterloo, ON, Canada) with the following parameters: mobility tolerance: 0.05 1/K0; mass tolerance: 50ppm; and retention time tolerance: 0.5min. PEAKS LFQ conducts a retention time correction based on a single sample within a control group and then checks this against a "training group" composed of replicates within a group. Differentially abundant proteins (>1.5 fold) were then exported as an excel file. Only proteins with at least 75% detection per animal were included in analyses.

SUPPLEMENTARY DATA

References

1. Vieira-Potter VJ, Padilla J, Park YM, Welly RJ, Scroggins RJ, Britton SL, Koch LG, Jenkins NT, Crissey JM, Zidon T, Morris EM, Meers GM, Thyfault JP: Female rats selectively bred for high intrinsic aerobic fitness are protected from ovariectomy-associated metabolic dysfunction. American journal of physiology Regulatory, integrative and comparative physiology 2015;308:R530-542
2. Wainright KS, Fleming NJ, Rowles JL, Welly RJ, Zidon TM, Park YM, Gaines TL, Scroggins RJ, Anderson-Baucum EK, Hasty AH, Vieira-Potter VJ, Padilla J: Retention of sedentary obese visceral white adipose tissue phenotype with intermittent physical activity despite reduced adiposity. Am J Physiol Regul Integr Comp Physiol 2015;309:R594-602
3. Huang ZH, Manickam B, Ryvkin V, Zhou XJ, Fantuzzi G, Mazzone T, Sam S: PCOS is associated with increased CD11c expression and crown-like structures in adipose tissue and increased central abdominal fat depots independent of obesity. The Journal of clinical endocrinology and metabolism 2013;98:E17-24
4. Srere PA: [1] Citrate synthase: [EC 4.1.3.7. Citrate oxaloacetate-lyase (CoA-acetylating)]. In *Methods in Enzymology*, Academic Press, 1969, p. 3-11
5. Grunewald ZI, Winn NC, Gastecki ML, Woodford ML, Ball JR, Hansen SA, Sacks HS, Vieira-Potter VJ, Padilla J: Removal of interscapular brown adipose tissue increases aortic stiffness despite normal systemic glucose metabolism in mice. Am J Physiol Regul Integr Comp Physiol 2018;314:R584-R597
6. Santa C, Anjo SI, Manadas B: Protein precipitation of diluted samples in SDS-containing buffer with acetone leads to higher protein recovery and reproducibility in comparison with TCA/acetone approach. Proteomics 2016;16:1847-1851
7. Link AJ, LaBaer J: Solution protein digest. Cold Spring Harb Protoc 2011;2011:pdb prot5569
8. Meier F, Beck S, Grassl N, Lubeck M, Park MA, Raether O, Mann M: Parallel Accumulation-Serial Fragmentation (PASEF): Multiplying Sequencing Speed and Sensitivity by Synchronized Scans in a Trapped Ion Mobility Device. J Proteome Res 2015;14:5378-5387

SUPPLEMENTARY DATA

Supplementary Figure S1. Effects of sympathetic denervation of iBAT at thermoneutrality
(A) Isolation and resection of 5 intercostal nerves that innervate iBAT.
(B) Representative confocal microscopy and Plin 1 immuno-stained images of intact vs denervated iBAT lobes
(C) iBAT mass intact vs denervated lobe (within animal) (n=8/lobe).
(D) iBAT protein expression with representative immunoblots in intact vs denervated lobes (n=8/lobe).
Data are mean ± SE.
*p<0.05 vs intact iBAT lobe.

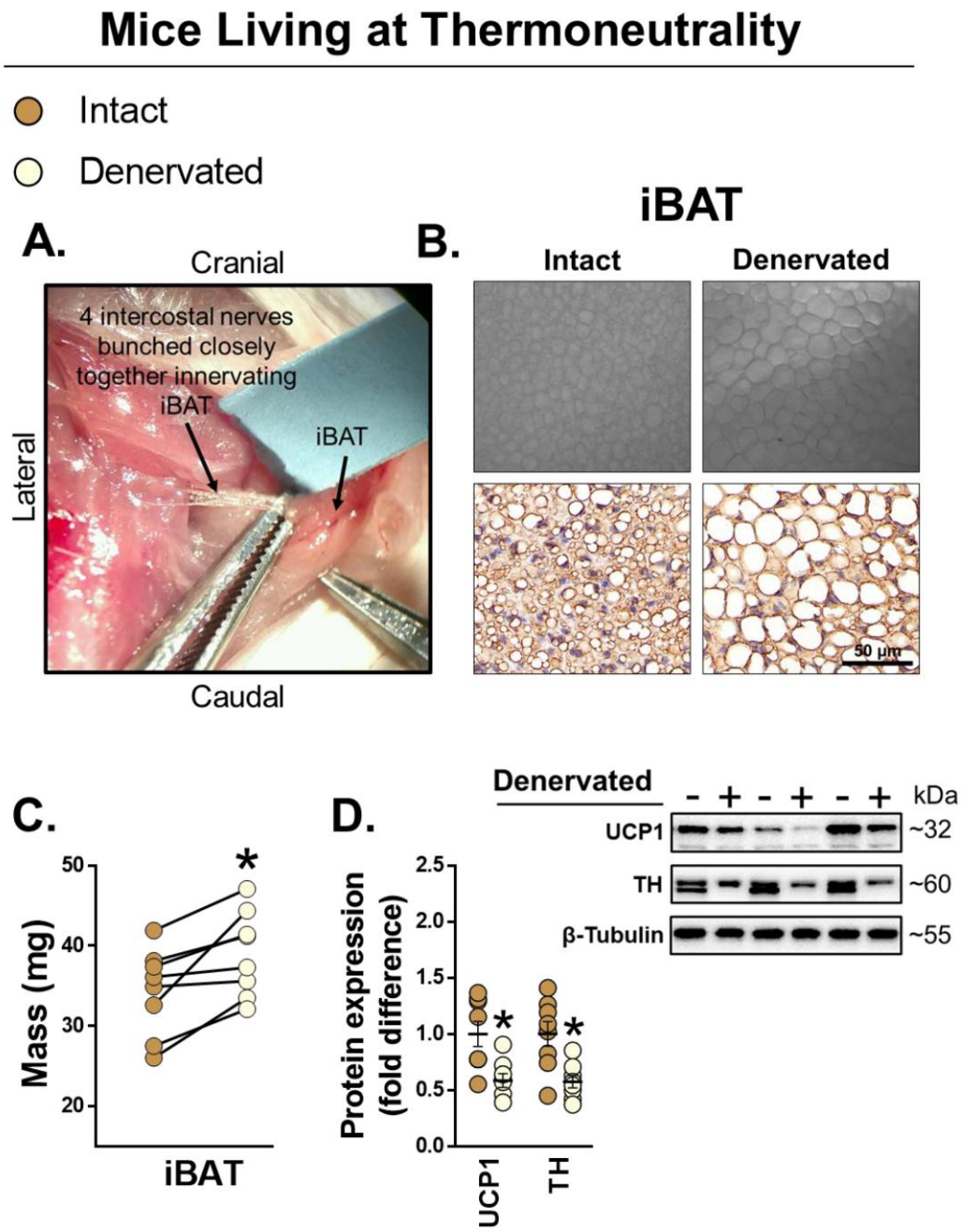

SUPPLEMENTARY DATA

Supplementary Figure S2. Effects of age and diet on metabolic function and BAT phenotype.
(A) Final body weight in 14-week-old and 24-week-old female mice consuming control diet (CD) or Western diet (WD) (n=6-10/group).
(B&C) Fat mass, lean mass, and BAT mass (n=6-10/group).
(D&E) Glucose tolerance test (GTT) and fasting insulin concentrations (n=6-10/group).
(F) Acute cold tolerance test (CTT). Baseline rectal temperature measurements were recorded in home cages (28°C). Thereafter, mice were placed in environmental cold chambers (4°) and rectal temperature measurements were taken every 30 min for 120 min (n=6-8/group).
(G) Representative Plin 1 immuno-stained images of iBAT.
(H) Mean protein expression and representative immunoblots from BAT. Mice consuming CD and WD were run on separate gels such that age comparisons from each respective diet were made within the same gel.

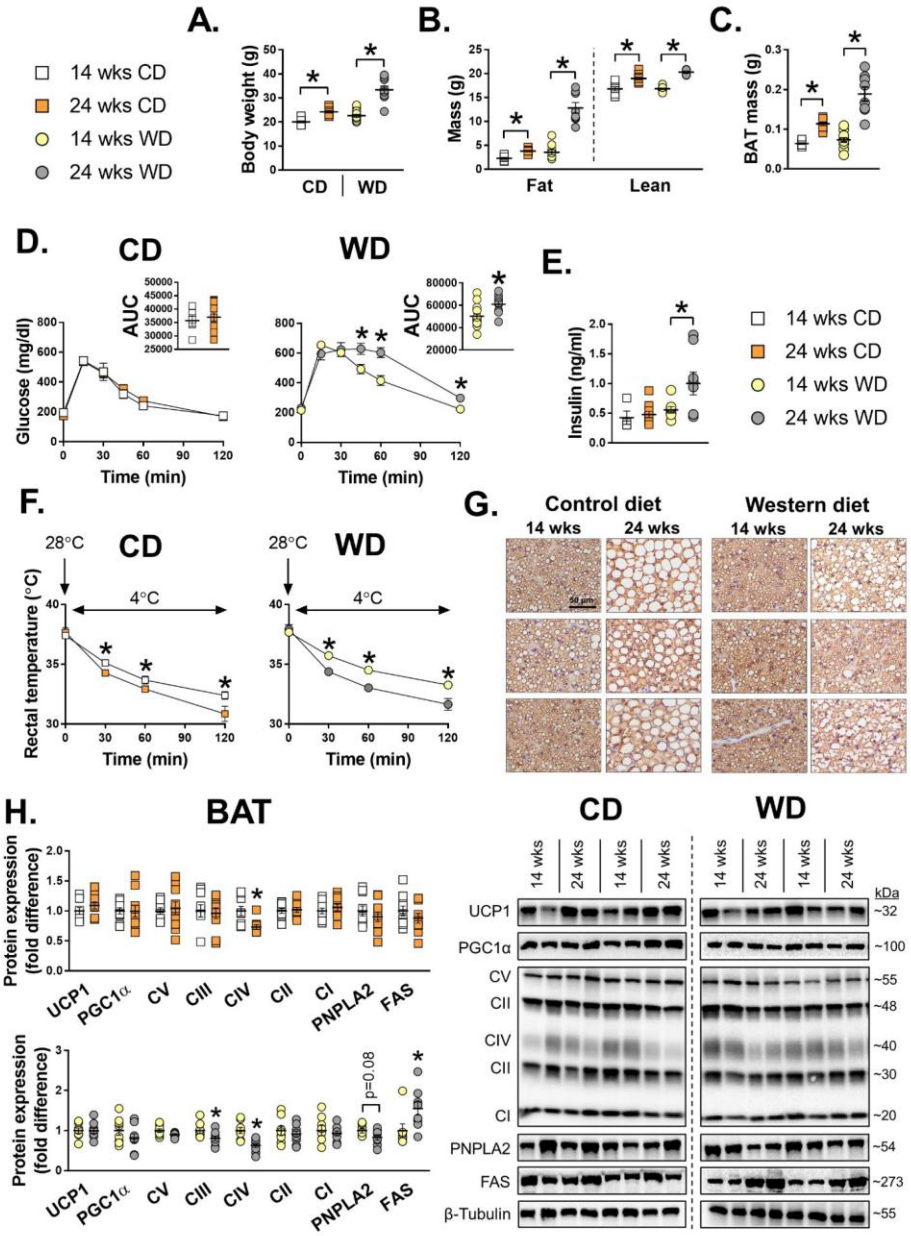

SUPPLEMENTARY DATA

Supplementary Table S1. Antibodies

Antibody	Source	Identifier/dilution
Rabbit anti-ACC	Cell Signaling Technology	Cat. #3662; 1:1000
Rabbit anti-phospho $ACC_{Ser\ 79}$	Cell Signaling Technology	Cat. #3661; 1:1000
Rabbit anti-UCP1	Millipore Sigma	Cat. #U6382; 1:1000
Rabbit anti-TH	Abcam	Cat. #ab112; 1:1000
Rabbit anti-PGC1α	Millipore Sigma	Cat. #516557; 1:1000
Mouse anti-OXPHOS cocktail	Abcam	Cat. #110413; 1:2000
Rabbit anti-β tubulin	Cell Signaling Technology	Cat. #2146; 1:1000
Rabbit anti-FAS	Cell Signaling Technology	Cat. #3189; 1:1000
Rabbit anti-HSL	Cell Signaling Technology	Cat. #4107; 1:2000
Rabbit anti-phospho $HSL_{Ser\ 660}$	Cell Signaling Technology	Cat. #4126; 1:2000
Rabbit anti-phospho HSL_{Ser563}	Cell Signaling Technology	Cat. #4139; 1:2000
Rabbit anti-perilipin	Cell Signaling Technology	Cat. #3470; 1:1000
Rabbit anti-Mac-2	Cedarlane	Cat. #CL8942AP; 1:1500
Rabbit anti-JNK	Cell Signaling Technology	Cat. #9252; 1:1000
Rabbit anti-phospho $JNK_{Thr183/Tyr185}$	Cell Signaling Technology	Cat. #9251; 1:1000
Rabbit anti-p38	Cell Signaling Technology	Cat. #9212; 1:1000
Mouse anti-phospho $p38_{Thr180/Tyr182}$	Cell Signaling Technology	Cat. #9216; 1:1000
Mouse anti-OPA1	BD BioScience	Cat. # 612606; 1:4000
Mouse anti-SDHA	Thermo Fisher Scientific	Cat. # 459200; 1:5000
Rabbit anti-actin	Abcam	Cat. # ab8227; 1:2000
Rabbit anti-IgG	Cell Signaling Technology	Cat# 7074; 1:2000
Mouse anti-IgG	Cell Signaling Technology	Cat# 7076; 1:2000

SUPPLEMENTARY DATA

Supplementary Table S2. Gene Primers

Gene	Forward	Reverse
18S	TCAAGAACGAAAGTCGGAGG	GGACATCTAAGGGCATCAC
Acc	CTGTATGAGAAAGGCTATGTG	AACCTGTCTGAAGAGGTTAG
Ccl2	CAAGATGATCCCAATGAGTAG	TTGGTGACAAAAACTACAGC
Cd11c	ATGCCACTGTCTGCCTTCAT	GAGCCAGGTCAAAGGTGACA
Cidea	TGCTCTTCTGTATCGCCCAGT	GCCGTGTTAAGGAATCTGCTG
F4/80	GTGCCATCATTGCGGGATTC	GACGGTTGAGCAGACAGTGA
Fas	GATTCAGGGAGTGGCTATTG	CATTCAGAATCGTGGCATAG
Fgf21	GTACCTTCTACACAGATGACGAA	CGCCTACCACTGTTCCATCCT
Hsl	CCGAGATGTCACAGTCAATGGA	CAGGCCGCAGAAAAAAG
Pgc1α	CCCTGCCATTGTTAAGACC	TGCTGCTGTTCCTGTTTTC
Pka	TGCCACGACTGACTGGATTG	GTCCCTTACTGGCTTGAGGA
Pnpla2	ATGCTGTGGAATGAGGACATAG	CATAGTGAGTGGCTGGTGAAA
Pparγ	CGGGCTGAGAAGTCA	TGCGAGTGGTCTTCCATCAC
Prdm16	CAGCACGGTGAAGCCATTC	GCGTGCATCCGCTTGTG
Ucp1	CACGGGGACCTACAATGCTT	ACAGTAAATGGCAGGGGACG

SUPPLEMENTARY DATA

Supplementary Table S3. *Experiment 1*: Tissue weights and body composition

	$CD_{28°C}$	$WD_{28°C}$	$WD_{20°C}$	ANOVA
Fat mass, g	2.3 ± 0.2	3.9 ± 0.5*	4.1 ± 0.2*	p=0.02
Lean mass, g	16.8 ± 0.4	16.9 ± 0.2	17.4 ± 0.3	p=0.43
%Fat mass	11.3 ± 1.0	17.1 ± 2.0*	17.7 ± 0.9*	p=0.03
BAT, g	0.06 ± 0.002	0.07 ± 0.005	0.07 ± 0.004	p=0.25
gWAT, g	0.30 ± 0.04	0.65 ± 0.09*	0.57 ± 0.04*	p=0.006
Heart, g	0.12 ± 0.01	0.11 ± 0.005	0.14 ± 0.006*#	p=0.005

*$p<0.05$ vs $CD_{28°C}$, #$p<0.05$ vs $WD_{28°C}$

SUPPLEMENTARY DATA

Supplementary Table S4. *Experiment 4*: BAT proteome differences by diet and physical activity

Protein Name	Principal Function	WD+WR vs. WD	CD vs. WD	WD+WR vs. CD
TCPH (T-complex protein 1 subunit eta)	Protein folding	↑	↑	↔
FTL1 (Ferritin light chain 1)	Iron transport/storage	↑	↑	↔
PON1 (Serum paraoxonase/arylesterase 1)	Lipid metabolism	↔	↓	↔
ACOD1 (Acyl-CoA desaturase 1)	Lipid metabolism	↔	↑	↔
APOC3 (Apolipoprotein C-III)	Lipid metabolism	↔	↓	↔
PRD13 (PR domain zinc finger protein 13)	Transcriptional regulation	↔	↔	↓
NLRP6 (NACHT, LRR and PYD domains-containing protein 6)	Innate immunity/inflammation	↑	↔	↔
ABLM3 (Actin-binding LIM protein 3)	Cytoskeleton organization	↑	↔	↔
MPI (Mannose-6-phosphate isomerase)	Mannose metabolism	↔	↔	↑
QCR8 (Cytochrome b-c1 complex subunit 8)	Mitochondrial respiratory chain	↔	↓	↔
FTH1 (Ferritin heavy chain)	Iron transport/storage	↑	↑	↔
APOE (Apolipoprotein E)	Lipid metabolism	↔	↔	↓
NOL3 (Nucleolar protein 3)	Apoptosis repressor	↔	↑	↔
PPR3F (Protein phosphatase 1 regulatory subunit 3F)	Glycogen metabolism	↑	↔	↔
ACLY (ATP-citrate lyase)	Fatty acid biosynthesis	↔	↑	↔
SAHH2 (S-adenosylhomocysteine hydrolase-like protein 1)	DNA replication/mRNA processing	↑	↑	↔
AFG1L (AFG1-like ATPase)	Mitochondrial morphology	↔	↓	↔
APOA4 (Apolipoprotein A-IV)	Lipid metabolism	↔	↓	↔

SUPPLEMENTARY DATA

ACACA (Acetyl-CoA carboxylase 1)	Fatty acid biosynthesis	↔	↑	↔
NUMA1 (Nuclear mitotic apparatus protein 1)	Spindle formation of chromosomes	↔	↔	↓
TCPD (T-complex protein 1 subunit delta)	Protein folding	↑	↑	↔
GALM (Aldose 1-epimerase)	Hexose metabolism	↑	↑	↔
ODBA (2-oxoisovalerate dehydrogenase subunit alpha, mitochondrial)	Amino acid metabolism	↔	↔	↓
MOT2 (Monocarboxylate transporter 2)	Lactate/pyruvate transport	↔	↓	↔
TBB2A (Tubulin beta-2A chain)	Cytoskeleton structure	↑	↑	↔
FBLN2 (Fibulin-2)	Extracellular matrix organization	↔	↓	↔
MYO9A (Unconventional myosin-Ixa)	Cell junction assembly	↔	↓	↔

↔, no change; ↓, decrease; ↑, increase